VII International Conference on Computational Methods in Marine Engineering
MARINE 2017
M. Visonneau, P. Queutey and D. Le Touzé (Eds)

NUMERICAL SIMULATION OF LARGE COMMERCIAL SHIP NAVIGATION ON PARANÁ RIVER, ARGENTINA

MARINE 2017

GERARDO FRANCK, SILVINA MANGINI, HÉCTOR PRENDE, JOSÉ HUESPE AND YASSER PALAY ESQUIVEL

Facultad de Ingeniería y Ciencias Hídricas
Universidad Nacional del Litoral
Ciudad Universitaria, 3000 Santa Fe, Argentina
e-mail: gerardofranck@yahoo.com.ar, silvinamangini@yahoo.com.ar
web page:http://fich.unl.edu.ar

Key words: Computational Methods, Post-Panamax sailing, Argentinean waterway

Abstract. In recent years, the large commercial ships (Post-Panamax) started sailing the Argentinean waterway of the Paraná River. So that, the research project of the FICH-UNL called "Analysis of Hydro-Sedimentological Effects Caused by River Navigation on Argentinean Waterways" decided to use the computational simulation as one of tools research to study the hydraulic and sedimentological effects caused by the navigation of these ships on the morphology of the rivers of the Argentine waterway.

One of the premises of this work was to explore the capabilities of the Adapco STAR CCM + CFD code to simulate the ship navigation in calm water in order to measure the heights of waves generated (among others), validating its results with the experimental one (physical model of large ships navigation carried out at the Hydraulics Laboratory of FICH-UNL).

Navigation situation simulated: JAPAN Bulk Carrier (JBC; Lpp: 280 m, Bwl: 45 m and D: 25 m) with a service speed of 22 knots (11,3m/s) navigating against a flow stream with velocity of 2m/s (habitual situation of JBC navigation on Paraná River).

The numerical modeling reproduced the navigation ship in scale (1/36.7), using a Computational Fluid Dynamics code (CFD) by finite-volume method (VOF). A study of mesh dependence was performed to analyze the convergence model. A mesh of hexahedral cells was used in the Volume of Fluid (VOF) Multiphase Model for waves and dumping waves. The turbulence was modeled by a k-Epsilon model from Reynolds Average. Wave damping was used in the lateral walls of the domain.

1 INTRODUCTION

This work presents one of the first tasks carried out within the Research Project of the FICH-UNL (Facultad de Ingeniería y Ciencias Hídricas, Universidad Nacional del Litoral) called "Analysis of Hydrosedimentological Effects Caused by River Navigation in Argentinean Waterways". The main purpose of this project is to quantify the hydraulic and sedimentological effects caused by ships navigation on the morphology of the rivers of Argentine waterway.

The waves and induced currents produced by the navigation of ships produce an increase of turbulence levels, fluctuating overpressures, shear forces and bed sediment transport, which

affect the natural morphology of the rivers and navigation channels.

The research focused on the development of four tasks, with the purpose of knowing the wave pattern and the maximum height of the wave produced by the ships navigation on the Argentine Waterway:

1- Study of existing expressions or, generation of new ones.
2- Development of a sensor to measure wave heights.
3- Physical and experimental simulation of Barge Train and Pos-Panamax ship at the Hydraulic Laboratory of FICH.
4- Numerical simulation of Pos-Panamax ship navigation in order to estimate the heights of waves generated (among others), since large ships are just beginning to navigate the Argentine waterway.

In recent years, computational techniques of fluid dynamics as CFD (Computational Fluid Dynamics), have been incorporated into optimization of simulation procedures for ship´s hull configuration, making the CFD simulations, an important tool for ship design and performance analysis.

Currently, we do not have empirical expressions to estimate the maximum wave height (Hm) for fast ships, such as the JBC, (situations with velocity and Froude number greater than 20 knots and 0.7 respectively), because the existing ones (Pianc and Sorensen, that are adaptable to navigational situations in our rivers), are valid for Froude numbers up to 0.7. Therefore, we try to incorporate the CFD as a tool to predict these behaviors and, at the same time, be able to explore the capabilities of the Adapco STAR CCM + CFD code on the numerical simulation of the JBC navigation in calm water.

The main purpose of this numerical simulation was to reproduce the wave pattern, from which, it can be estimated height of waves generated by the fast navigation of the JBC, at different distances from the navigation line.

In the present work, are presented one of the first results of the numerical simulation of unsteady turbulent flow around a fast ship (JBC), navigating in calm (state that is an exception in the case of marine situations) and deep water. Even though, the deep water conditions used in this simulation do not faithfull represents the characteristics of navigation in rivers, it facilitates the simulation, achieving stable, with good results in terms of the goal pursued. Numerical analyses are done by means of RANS solution and the well-known standard k-ε two equation turbulence model was used as turbulence model.

The validation of the numerical modeling was made from physical and experimental model results of the same navigation situation

2 NUMERICAL MODELLING

2.1 Ship geometry and conditions

In this study, it was simulated the navigation of JBC Bulk Carrier (Figure 1) on calm water in a scale of 1/36.7. The numerical simulated situation was a JBC with a service speed of 22 knots (11,3 m/s) navigating against a flow stream with velocity of 2 m/s (Habitual situation of JBC navigation on Paraná River). The main properties of the geometry are depicted in Table 1. Service speed of JBC in numerical simulation and full scale and, their correspond ship´s Froude number for the JBC navigation are shown in Table 2.

Figure 1: JBC Bulk Carrier

Table 1: Main properties of JBC geometry

Main particulars		**Full scale**	**Model scale (1:36,7)**
Length between perpendiculars	L_{PP} (m)	280	7.62
Length of waterline	L_{WL} (m)	285	7.76
Maximum beam of water line	B_{WL} (m)	45	1.22
Depth	D (m)	25	-
Draft	T (m)	14	0,38
Displacement volume	∇ (m^3)	151369	6,54
Block coefficient (CB)	$\nabla /(L_{PP}B_{WL}\ T)$	0.8581	0.8581

Table 2: Service speed and Froude ship number (Fn_{ship})

	U: Ship velocity (m/s)	V: Velocity current (m/s)	Fn_{ship}
Full scale	11.3	-2	0.253
Numerical Model Scale	1,86	-0,33	0,253

2.2 Governing equations

For incompressible flows without body forces, the averaged continuity and momentum equations may be written in tensor form and Cartesian coordinates as follows [3]:

$$\frac{\partial \rho \bar{u}_i}{\partial x_i} = 0; \qquad \text{for the continuity} \tag{1}$$

$$\frac{\partial(\rho \bar{u}_i)}{\partial t} + \frac{\partial}{\partial x_j}\left(\rho \bar{u}_i \bar{u}_j + \rho \overline{u'_i u'_j}\right) = \frac{\partial \bar{P}}{\partial x_i} + \frac{\partial \bar{\tau}_{ij}}{\partial x_j}; \text{ for the momentum equations} \tag{2}$$

in which $\bar{\tau}_{ij}$ are the mean viscous stress tensor components, as shown in Equation (3)

$$\bar{\tau}_{ij} = \mu\left(\frac{\partial \bar{u}_i}{\partial x_j} + \frac{\partial \bar{u}_j}{\partial x_i}\right) \tag{3}$$

Where P is the mean pressure, $\bar{u}_i$ is the averaged components of the velocity vector, $\left(\rho \overline{u'_i u'_j}\right)$ is the Reynolds stresses, μ is the dynamic viscosity and ρ is the fluid density. To model the fluid flow, it was used a solver employed with finite volume method, which discretizes the integral formulation of the Navier– Stokes equations. The RANS solver employs a predictor–corrector approach to link the continuity and momentum equations. The eddy viscosity ν_t is calculated by combining turbulent kinetic energy, *k*, and the rate of dissipation of the turbulent energy ε. The standard *k*-ε two equation turbulence model has been used to simulate the turbulent flows. Where turbulent Prandl numbers used σ_k=1 y σ_ε=1.2; and $C_{\square}$= 0.09; $C_{\varepsilon 1}$= 1.44 and $C_{\varepsilon 2}$= 1.9.

2.3 Physics modelling

A standard k–ε model was used as the turbulence model (extensively used for many industrial applications [1] and considered as economical in terms of CPU time [5]). The "Volume of Fluid" (VOF) method was used to model and position the free surface, either with a flat or regular wave. The VOF method is considered as "a simple multiphase model, very convenient to simulating flows of several immiscible fluids on numerical grids capable of resolving the interface between the mixtures phases" [1]. This model has high numerical efficiency and suitable for simulating flows in which each phase forms a large structure, with a low contact area between them. The VOF model is based on the assumption that the same basic governing equations used for a single phase problem can be solved for all the fluid phases of the domain, assuming the same velocity, pressure and temperature. Therefore, the equations are solved for an equivalent fluid whose properties represent the different phases and independent volume fractions [1]. The input velocity and volume fraction of both phases in each cell and the output pressure are all functions of the plane wave or regular wave used to simulate the free surface. The free surface is not fixed; it is dependent on the specifications of this flat or regular wave, with the VOF model making calculations for both the water and air phases. In this work, a second-order convection scheme was used throughout all simulations in order accurately capture sharp interfaces between the phases. In the Figure 2, the free surface was represented by showing the water volume fraction profile on the hull, a value of 0.5 for the volume fraction of water implies that a computational cell is filled with 50% water and 50% air. This value therefore indicates the position of the water–air interface, which corresponds to the free surface.

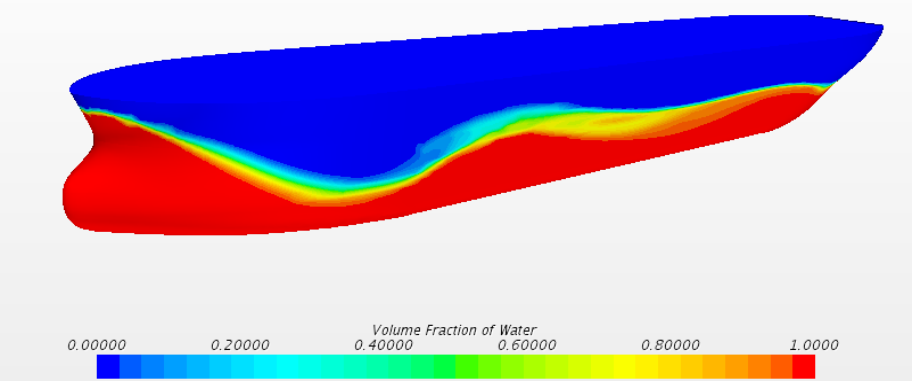

Figure 2: Free Surface representation on the ship hull

In this work, the segregated flow model, which solves the flow equation in an uncoupled manner, was applied throughout all simulations in the RANS solver. The grid is must be simply refined in order to enable the variations in volume fraction to be more accurately captured.

2.4 Computational domain and boundary condition

The computational domains were created mainly to see the waves producing by the ship navigation in calm water. In the domains, an overset mesh was used to facilitate the motions of the full-scale ship model.

The determination of these boundary conditions is of critical importance to obtain accurate solutions. The selection of the appropriate boundary conditions can prevent unnecessary computational costs when solving the problem [2].

The boundary conditions in the domain for this simulation (calm water) were the ones depicted in Figure 3. The computational domain extends from -2.2 Lpp < x <1.2 Lpp, 0< y <1.5 Lpp and -2.25 Lpp < z <1.15 Lpp, where half of the entire computational domain was taken into account due to vertical plane symmetry. The ship axis is located along the x-axis, with the bow located at x = Lpp and the stern at x = 0. The still water level lies at z = 0.

A general view of the computation domain with the JBC hull model and the notations of selected boundary conditions are depicted in Figure 3.

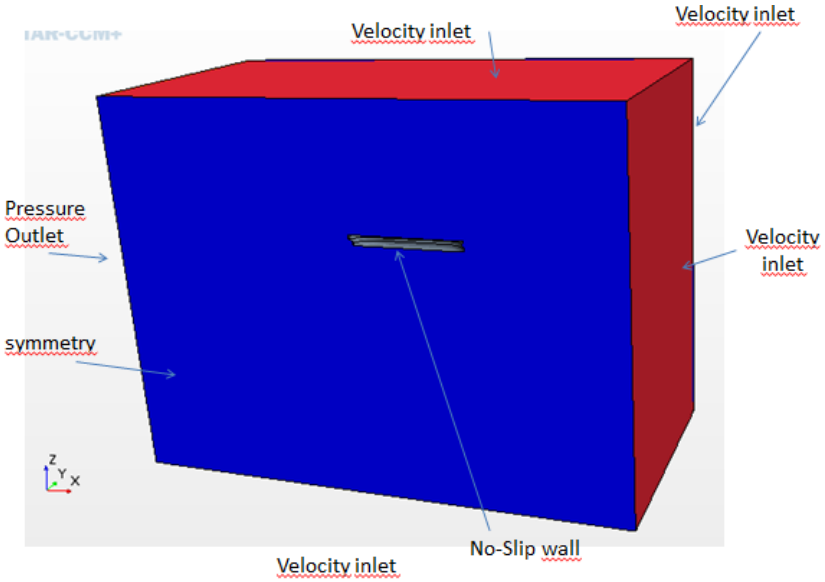

Figure 3: Boundary conditions in the simulation domain

In order to reduce computational complexity and demand, only half of the hull is represented. A symmetry plane forms the centerline domain face. The velocity inlet (-2.19 m/s) boundary condition was set in the negative direction x and the positive x direction was modeled as pressure outlet.

The top and bottom boundaries were both selected as velocity inlet. The symmetry plane has a symmetry condition, and the side of the domain (the negative y direction) has a velocity inlet boundary condition as well. The use of the velocity inlet boundary condition at the top and the side of the background prevents the fluid from sticking to the walls, so this prevent a velocity gradient from occurring between the fluid and the wall. Hence, the flow at the very top and very side of the background is also directed parallel to the outlet boundary, this enables to be prevented fluid reflections from the top and side of the domain. The selection of the velocity inlet boundary condition for the top and bottom (deep water and infinite air conditions), do not faithfull represents the characteristics of navigation in rivers, however facilitate the simulation, achieving a stable simulation, with good results in terms of the objective pursued in this study (obtaining a wave pattern and height of waves, see Validation and Verification).

The waves generated by the presence of the JBC were treated by applying a numerical damping beach with a damping length of 5m (VOF wave damping capability of STAR-CCM+). This numerical beach model was used in downstream and transverse directions to

prevent reflections effects of waves. The pressure outlet boundary condition was set behind the ships to prevent back flow occurring and fixes static pressure at the outlet.

2.5 Mesh Generation

Mesh generation was performed using the automatic meshing facility in STAR-CCM+, which uses the Cartesian cut-cell method. A trimmed cell mesher was employed to produce a high-quality grid for complex mesh generating problems. The ensuing mesh was formed primarily of unstructured hexahedral cells with trimmed cells adjacent to the surface.

The computation mesh has areas of progressively refined mesh size in the area immediately around the hull, in the expected free surface and in the wake produced by the ship, in order to capture the complex flow features appropriately. Volumetric controls were using to refine the mesh density in these zones. The mesh was rigid, unstructured and body-fixed; in order to the motions of the body agree to the movement of grid points. The most refined mesh areas around the hull remained within the boundaries of the overset domain. The mesh had areas with refined progressively mesh size, around the hull, on the expected free surface, near the stern, near the bow and in the wake produced by the ship navigation. These refined mesh area allow that the complex flow features were appropriately captured. When generating the volume mesh, an extra care was given to the overlapping zone between the background and overset regions.

It is necessary to do a grid refinement study in order to estimate the grid related uncertainty. Therefore, for the numerical solution of the governing equations the domain was discretized in two different resolutions as coarse (807137) and fine (3,091.741 still running). The numerical grid system employed for the coarse grid with a general view of the computational domain and overset regions is shown in Figure 4. The coarse mesh grid had a range of cell sizes between 0.007 mts (refined grid) to 0.45 mts.

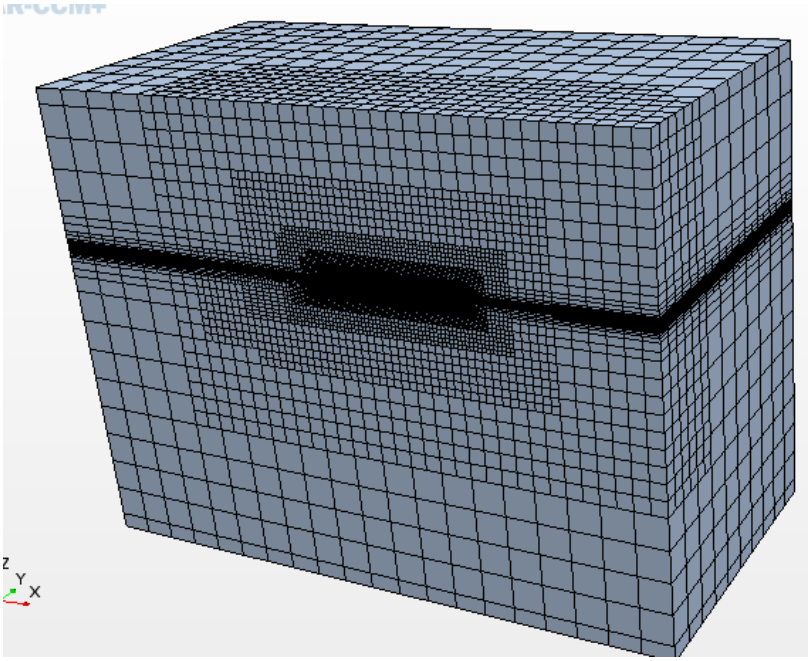

Figure 4: A general view of the background and overset regions and the applied boundary conditions.

Figure 5a shows a cross-section of the computation mesh where it can see clearly the refinement to capture the Kelvin wake. Figure 5b shows the surface mesh on the hull.

a 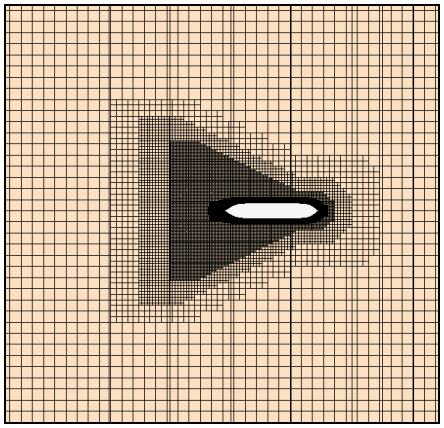 b 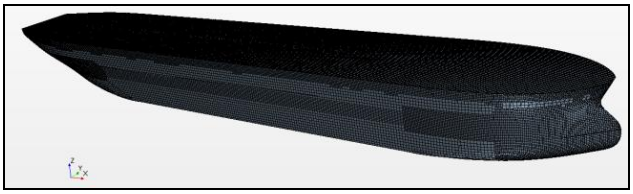

Figure 5: **a**: Cross-section of the computation mesh showing with refined mesh to capture the Kelvin wake. **b**: Surface mesh on the hull.

2.6 Choice of de time step

The Courant number (CFL), which is the ratio of the physical time step (Δt) to the mesh convection time scale, relates the mesh cell dimension Δx to the mesh flow speed U as: $CFL = U\,\Delta t/\Delta x$. The Courant number is typically calculated for each cell and should be less than or equal to 1 for numerical stability.

Often, in implicit unsteady simulations, the time step is determined by the flow properties, rather than the Courant number. For resistance computations in calm water, the time step size is determined by $\Delta t=0.005–0.01L/U$ (where L is the length between perpendiculars) in accordance with the related procedures and guidelines of [5]. The Navier-Stokes equations were dicretized by mean of first-order temporal scheme. The physical time step choiced was 0.04 seconds.

2.7 Wall Functions treatment

The wall functions are a set of semi-empirical functions used to satisfy the physics of the flow in the near wall region. Turbulence is affected in many ways by the presence of the wall through the non-slip condition that must be satisfied at the wall. Four areas in the near wall region are defined, the laminar sub-layer, the blending region, the log law region and the outer region. Each region has a different effect on turbulence and a particular care must be taken to the y+ position of the first cell in the boundary layer. A different set of equations will be used depending on the size of this cell but however this one must not be comprised between y+=5 and y+=30 because no turbulent model is available in this area. Instead of not resolving the entire boundary layer for a y+ comprised in the viscous sub-layer and buffer layer, wall functions are used to bridge the viscosity-affected region between the wall and the fully-turbulent region, [1].

The All-y+ wall treatment is a hybrid treatment that attempts to emulate the high- wall treatment for coarse meshes and the low-y+ wall treatment for fine meshes. It is also

formulated with the desirable characteristic of producing reasonable answers for meshes of intermediate resolution (that is, when the wall-cell centroid falls within the buffer region of the boundary layer), [1]. Two-Layer All y+ Wall Treatment is a formulation that is identical to the All y+ Wall Treatment, but contains a wall boundary condition for ε that is consistent with the two-layer formulation. This treatment is the recommended wall treatment where provided [1].

All the y+ values for the coarse grids can be seen on Figure 6 and the number of grid points and average y+ values are given in Table 3.

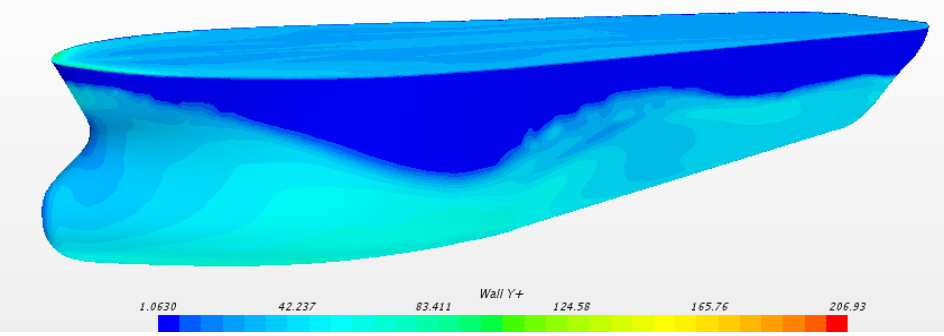

Figure 6: y+ values for the coarse grids.

Table 3: Number of grid points and average y+ values.Coarse Grid

Grid points number	average y +
807137	104.03

3 RESULTS

The following section will outline the simulation results achieved during this study, and will also provide some comparison with experimental results.

3.1 Wave Pattern

Figure 7 shows the volume fraction of air plot and the wave elevation at the bow and at the stern produced by the navigation of JBC, after the simulation has completed its run (solution time: 152 seconds, CPU time: 98.3 hours).

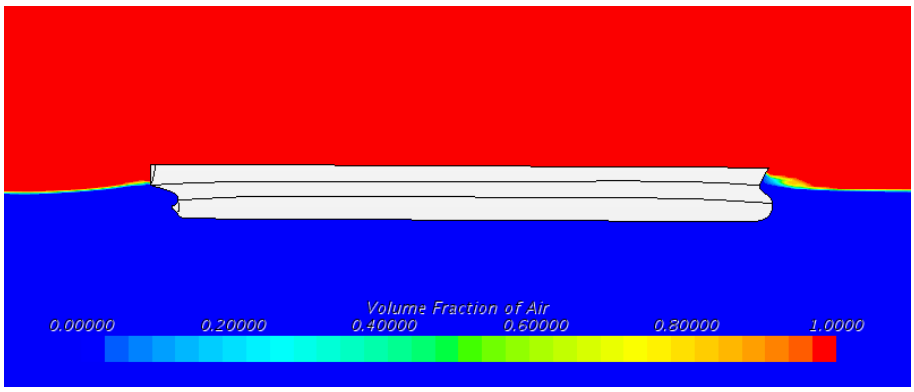

Figure 7: Volume fraction of air after the simulation has completed its run

Figure 8 shows both a plant view of global wave pattern generated by the JBC navigation, (after the simulation has completed its run) and the locations of logitudinal cuts of the wave pattern (isosurfaces scene) from which were obtained the longitudinal profiles of waves.

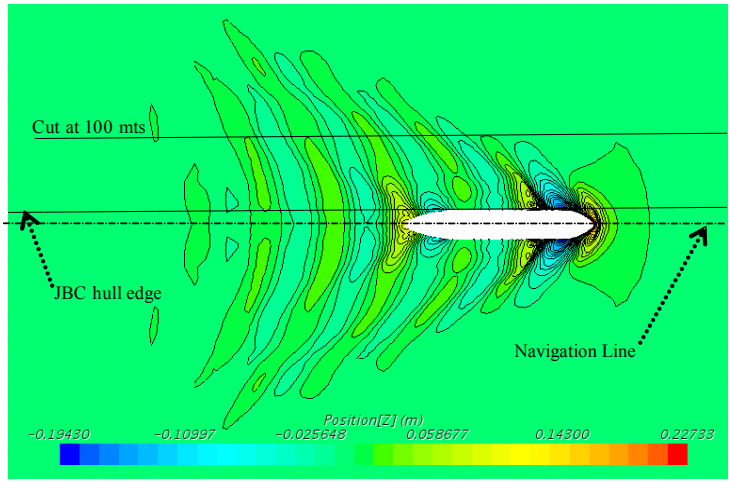

Figure 8: Wave pattern after the simulation has completed its run. Scheme of wave pattern cut to obtain logitudinal profiles of waves at 100mts of JBC hull edge.

Figure 9 shows the longitudinal profiles of water free-surface deformation at JBC hull contour and the logitudinal profile of wave cut at 100 m from the hull edge. In this Figure, can be appreciated in each profile, the maximum deformation of water free-suface at the contour hull and the maximun amplitude of the wave (Hm) at 100 m, which were estimated from the position (z in m) indicated by the color scale.

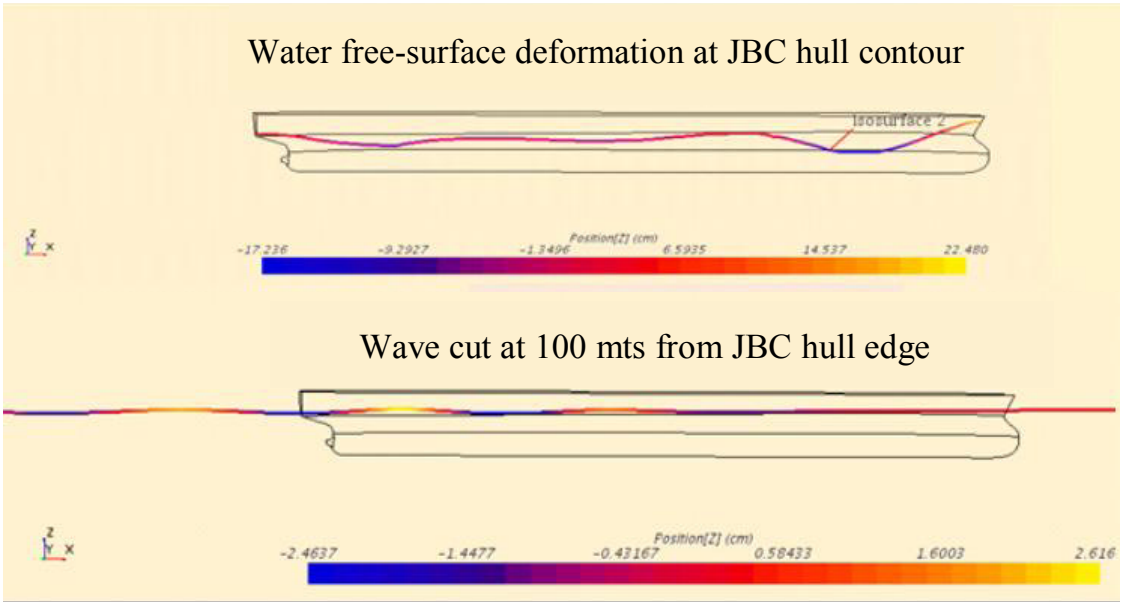

Figure 9: Logitudinal profile of water free-surface deformation at JBC hull contour and logitudinal profiles of waves at 100 mts from the JBC hull edge.

Table 4 shows the maximum amplitude of water free-surface deformation at JBC hull contour and the maximum waves height (Hm) at from JBC hull edge produced by the JBC navigation in the simulation model and its corresponding value in full scale.

Table 4: Maximum water free-surface deformation at ship contourn and maximum waves height (Hm) at 100 m from JBC hull edge.

	Maximum water free-surface deformation at JBC hull contour	Hm at 100 m
Numerical Model (E: 1:36.7)	0.39716 m	0.0508 m
Full scale	14.31 m	1.86 m

4 VALIDATION AND VERIFICATION

The results of the numerical simulation were compared with the results of an experimental physical model on scale (1:127). Based on the similarity of the Flow Froude number between the physical model and full scale (F=0.841), the physical model reproduced the same ship (JBC) navigation condition simulated in the computational model already presented, but, in rivers navigation conditions of Argentine Waterway (Shallow Water). The test was conducted in a laboratory channel of FICH, Figure 10.

On the physical model, waves produced by the ship navigation were estimated (from video images analysis) on three scales placed at distances of 0.79 m (100 in full scale), 1.58 m (200 m in full scale), and 2.37 m (300 m in full scale), see Figure 10.

Table 5 shows the characteristics of the simulated situation in the physical model and the maximum height of the wave measured at 0.79 m (100 m in full scale) produced by the ship navigation, and, Figure 10 shows images obtained during the experiment.

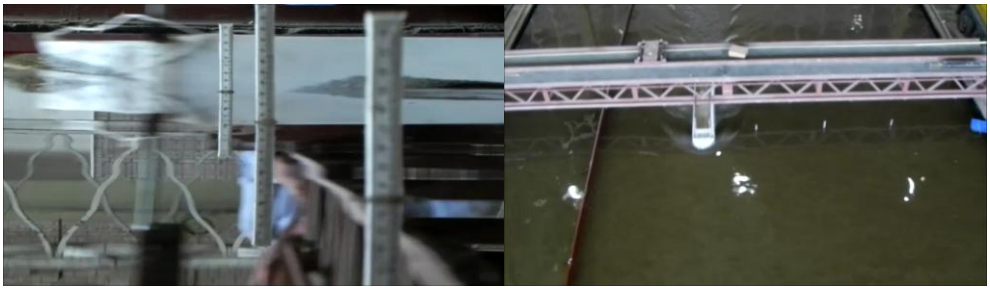

Figure 10: Images of the physical model during the test performance

Table 5: Characteristics of simulated navigation situation in the physical model.

Length (m)		Beam (m)		Height (m)		Draft (m)		Depth (m)		Ship velocity (m/s)		Scale location from the ship edge (m)		Height measured on the scale. Hmax (m)	
Model	Full Scale	Model	Full Scale	Model	Full Scale	Model	Full Scale	Model	Full Scale	Model	Full Scale	Model	Full Scale	Model	Full Scale
2.2	280	0.356	45	0.196	25	0.11	14	0.2	26	1,178	13.3	0.79	100	0.015	1.94

In Figure 11, a perspective view shows good match between the bow wave patterns around the ship hull of computational and physical models. Both models images also show a similar thin water elevation close to the bow.

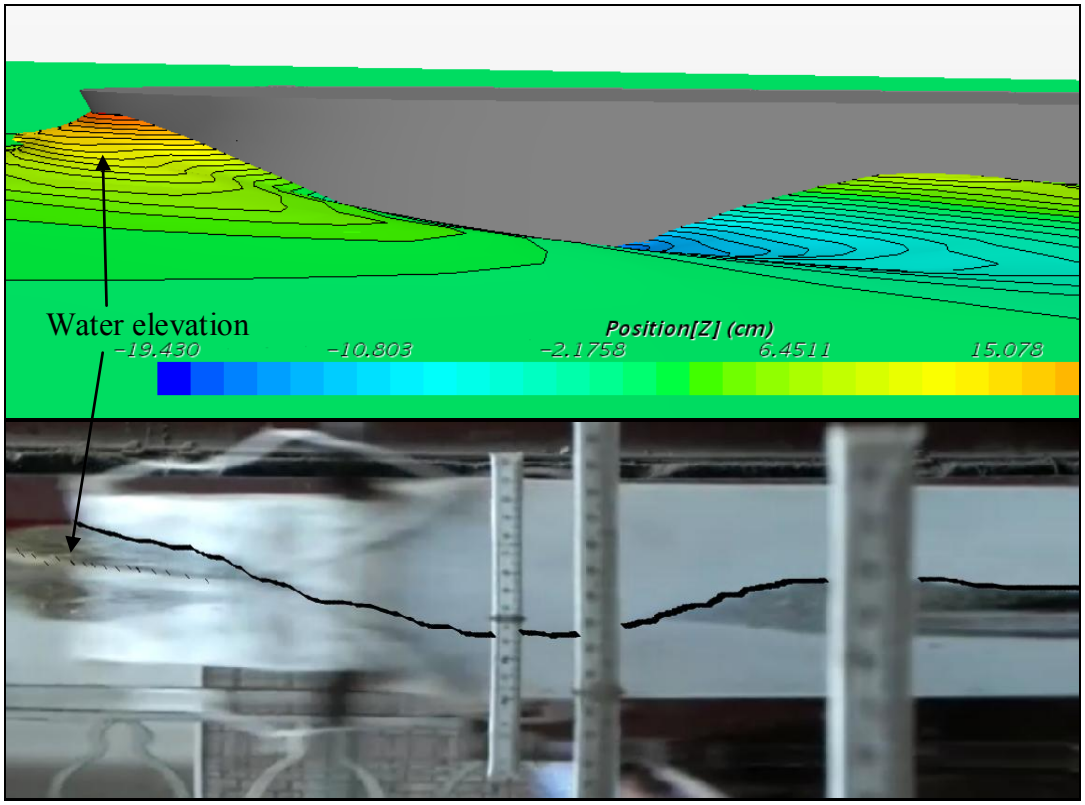

Figure 11. Perspective view of the bow wave patterns of computational and experimental models. (Fn_{ship} : 0.253)

For the scale of numerical simulation, the theoretical dynamic height of the water at the ship bow is given by: $V^2/2g$ (since the ship remains still facing a flow with a given inlet velocity). Being the flow velocity inlet of -2.19 m/s, the theoretical dynamic height results of 24.4 cm. The maximun heigth of water at the ship bow in the numerical simulation resulted of 23.705 cm (see Figure 12).

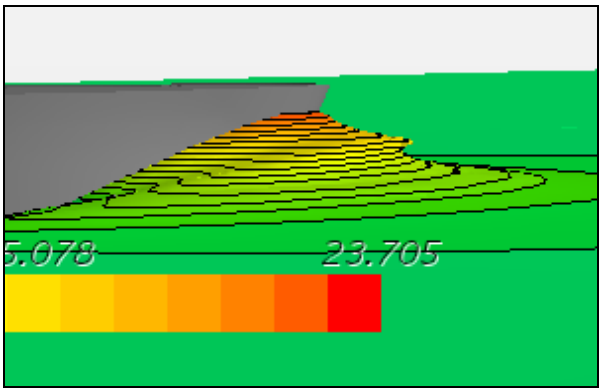

Figure 12. Heigth of water at the bow at the end of computational simulation.

5 CONCLUSIONS

The comparison of results between computational and experimental simulation of JBC navigation, for the simulated navigation conditions (Fn_{ship}= 0.253), shows that:

- Star CCM + predicts satisfactorily the free surface flow around the ship hull, navigating in shallow waters (Paraná Waterways), even thought, deep water boundary conditions are used in the simulation.
- The maximum wave height at 100 m from the hull side, obtained from computational model (Hm=1.86 m in full scale) and experimental model (1.94 mts in full scale) were very close (error: 4%).
- An error of 2.8% arises from the comparation between the theoretical dynamic height of water at the ship bow and the heigth of water observed at the ship bow in the numerical simulation.

For the above reasons, the numerical simulation (STAR CCM+ CFD) could be considered as a useful tool to predict free surface flows (waves) generates by ship navigation. Even using a coarse mesh (807139 cells), the comparison of results between both models (numerical and physical) was acceptable.

It is suggested to perform news numerical and experimental simulations of JBC navigation at different velocities, and, use finer for numerical simulation.

The computational simulation with a finer mesh (3,091.741 cells) for the same navigation situation of JBC is actually running.

6 REFERENCES

[1] CD-Adapco, 2014. User guide STAR-CCM+ Version 9.0.2.

[2] Date, J.C., Turnock, S.R., 1999. A Study into the Techniques Needed to Accurately Predict Skin Friction Using RANS Solvers with Validation Against Froude's Historical Flat Plate Experimental Data. University of Southampton, Southampton, UK p. 62 (Ship Science Reports, (114))

[3] Ferziger, J.H., Peric, M., 2002. Computational Methods for Fluid Dynamics, (Third Edit.) Springer, Berlin, Germany

[4] International Towing Tank Conference (ITTC), 2011b. Practical guidelines for ship CFD applications. In: Proceedings of the 26th ITTC.

[5] Querard, A.B.G., Temarel, P., Turnock, S.R. 2008. Influence of viscous effects on the hydrodynamics of ship-like sections undergoing symmetric and antisymmetric motions, using RANS. In: Proceedings of the ASME 27th International Conference on Offshore Mechanics and Arctic Engineering (OMAE), Estoril, Portugal, pp. 1–10